Precambrian Research, 50 (1991) 269–282
Elsevier Science Publishers B.V., Amsterdam

A cleavage triple point and its meso-scopic structures: the Mustio Sink (Svecofennides of SW Finland)

Reinoud P. Veenhof[1] and Harm Stel
Institute of Earth Sciences, Free University, de Boelelaan 1085, 1081 HV Amsterdam, The Netherlands

(Received March 29, 1990; accepted after revision November 13, 1990)

ABSTRACT

Veenhof, R.P. and Stel, H., 1991. A cleavage triple point and its meso-scopic structures: the Mustio Sink (Svecofennides of SW Finland) Precambrian Res., 50: 269–282.

A cleavage-triple-point (CTP) structure is analyzed, located at the west side of the Mustio gneiss dome in the Svecofennides of southwest Finland. The presence of the CTP and the pattern of mesoscopic fold structures exclude the origin of the Mustio dome by successive interference of fold phases. The highly variable deformation structures are explained in a single-phase deformation model by using the theoretical specific strain environments of a CTP. These environments are (1) horizontal oblation on top of a dome, (2) transition from horizontal to vertical oblation on the flanks of a dome, and (3) vertical constriction in the center of the CTP. It is shown that each strain environment is associated with specific development of foliation, folds, mesoscopic fold interference and strain intensity. The theoretical strain environments are confirmed by strain analysis.

Introduction

In this paper, the evolution of the Mustio mantled gneiss dome in the Svecofennides of southwestern Finland, is analyzed with reference to two models: (1) interference of successive cylindrical folds, or (2) single phase non-cylindrical doming. Mapping of the triangular synform west of the dome reveals a cleavage triple point (CTP; Brun et al., 1981) structure of S_1 foliation (to be referred to as Mustio sink, Figs. 1 and 2). The occurrence of CTP's was predicted by Gorman et al. (1978) and Ramberg (1981), modelled by Dixon and Summers (1983) and first mapped by Brun et al. (1981) in the Finnish Karelides. Its main characteristic is a tri- or multi-angular foliation pit which steepens towards the center (Fig. 2). The strain fields range from vertical constriction in the center through foliation parallel oblation at the flanks, towards pure horizontal oblation at the top of a dome. At least three interfering rising bodies are required to create a triple point. At the onset of doming, the cover will passively rotate or actively slide into the forming sink. At this stage, a horizontal flattening field (with concurrent foliation fabric development) will develop on top of the culminating domes or antiforms and will radially spread (Dixon, 1975). As the sink progressively develops, a horizontal compression field will develop in the center of the sink. It originates as bi-axial compression in the center and migrates progressively towards uniaxial horizontal compression at the flanks of the CTP. This horizontal compression will overprint (Dixon and Summers, 1983) the previously developed horizontal flattening field,

[1]Present address: International Tectostrat Geoconsultants BV, De Boelelaan 7, 1083 HJ Amsterdam, The Netherlands.

0301-9268/90/$03.50

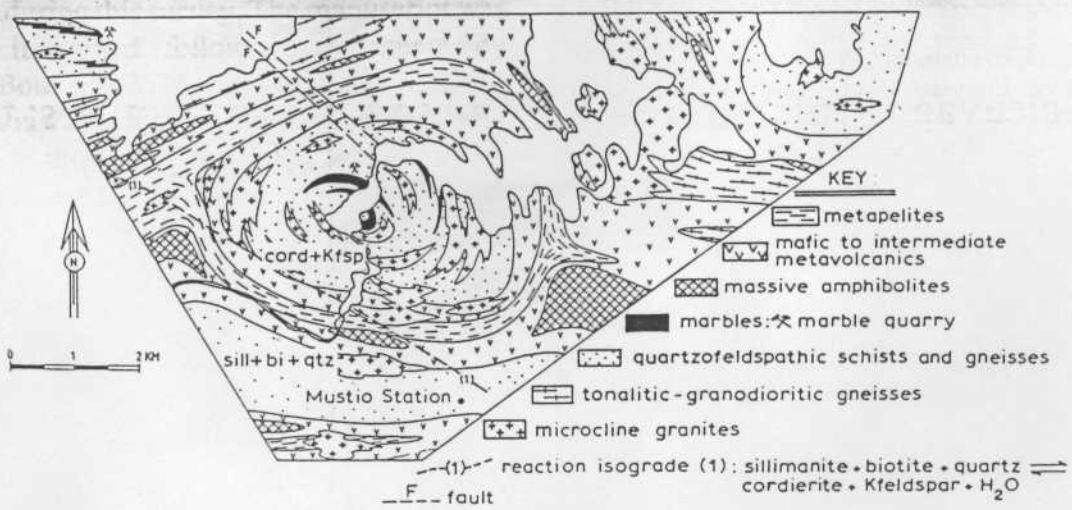

Fig. 1. Simplified geological map of the Mustio dome. Note the lithological symmetry on the limbs of the dome. Reaction isograd (1) represents a wide reaction zone rather than a uni-variant boundary. See Fig. 3 for location of the map. (After Bleeker and Westra, 1987).

more or less halfway between the center of the domes and CTP [i.e., the short axis (Z) of the strain ellipsoid changes from vertical to horizontal]. Hence, during the development of domes and sink, three different strain domains occur:

- progressive horizontal oblation at the top of the domes (zone 1);
- transition from horizontal to vertical oblation at the flanks of the CTP (zone 2);
- progressive vertical constriction in the center of the CTP (zone 3).

The presence of the CTP with its specific pattern of foldaxes in the Mustio area, excludes the origin of the Mustio dome by successive fold interference. Instead, its zonal strain distribution allows to explain the various generations and types of folding, by one-phase interdomal progressive deformation.

Doming is used here as a descriptive term. Several processes can lead to doming, e.g. ballooning (Bateman, 1984, 1986), buoyancy (Griffin, 1979; Dixon, 1975) or crossfolding, either simultaneous or successive (Park and Bowes, 1983). Criteria to distinguish the various processes have been raised and rejected (Coward, 1981; Bateman, 1984). The most difficult distinction concerns simultaneous cross-buckling or buoyancy of low density and low viscosity layers at depth, i.e., the distinction between a compressional, tensional or non-deviatoric stress field. Virtually, no criteria exist (Van den Eeckhout et al., 1986), except on the distribution of the total strain pattern. Obviously, the Mustio dome formation is related to the occurrence of a migmatized core, but whether this dome is a simultaneously "cross-buckled" migmatized rock-column or a buoyancy-driven structure, is difficult to ascertain. The minor deformational structures associated with the various processes will essentially be the same.

Geological setting

The Mustio dome is situated in the Kemiö–Orijärvi–Lohja–Järvenpää (KOLJ) supracrustal gneiss and schist belt (Fig. 3). It is part of the Svecofennian belt (1900–1880 Ma; Gaal and Gorbatschev, 1987) in which these late orogenic granitic domes occur abundantly (Simonen, 1980). The structure consists of intermediate to mafic volcano-sedimentary basal series, overlain by argillaceous sediments (Si-

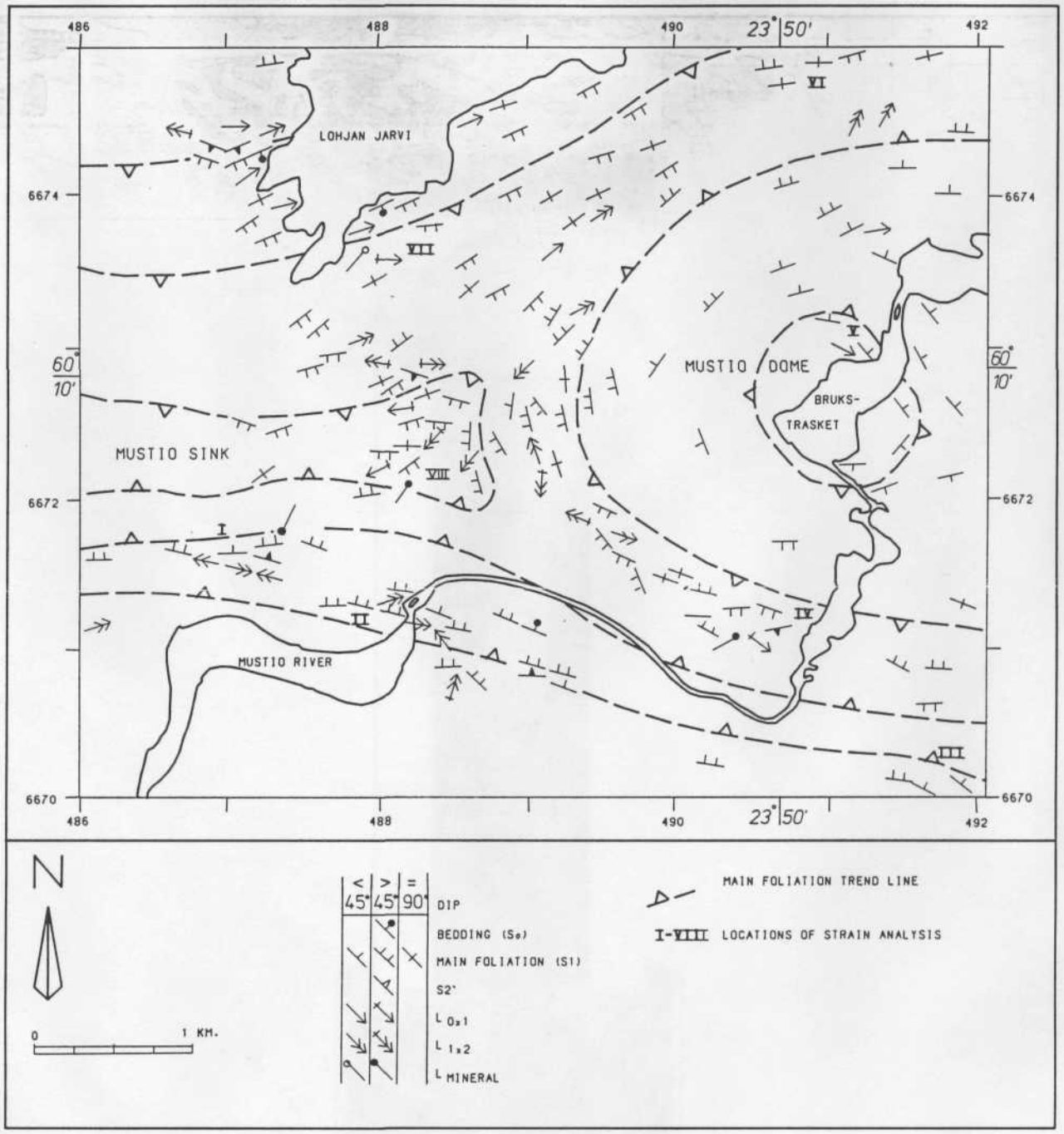

Fig. 2. Form surface and structural map of the Mustio sink. Note the triangular pattern of the main foliation and the steep dip of S_1 in the center of the synform. The locations of strain analysis (I–VIII) are indicated. See text for further discussion.

monen, 1980); the core of the dome is migmatized and intruded by microcline granites (Fig. 4). The KOLJ belt has been interpreted to represent an ancient island-arc setting (Gaal, 1982). However, its basement has to be discovered yet.

Petrography and metamorphism

According to the general stratigraphy of the Svecofennides (Simonen, 1980 and the mapping of Härme (1953) and Bleeker and Westra

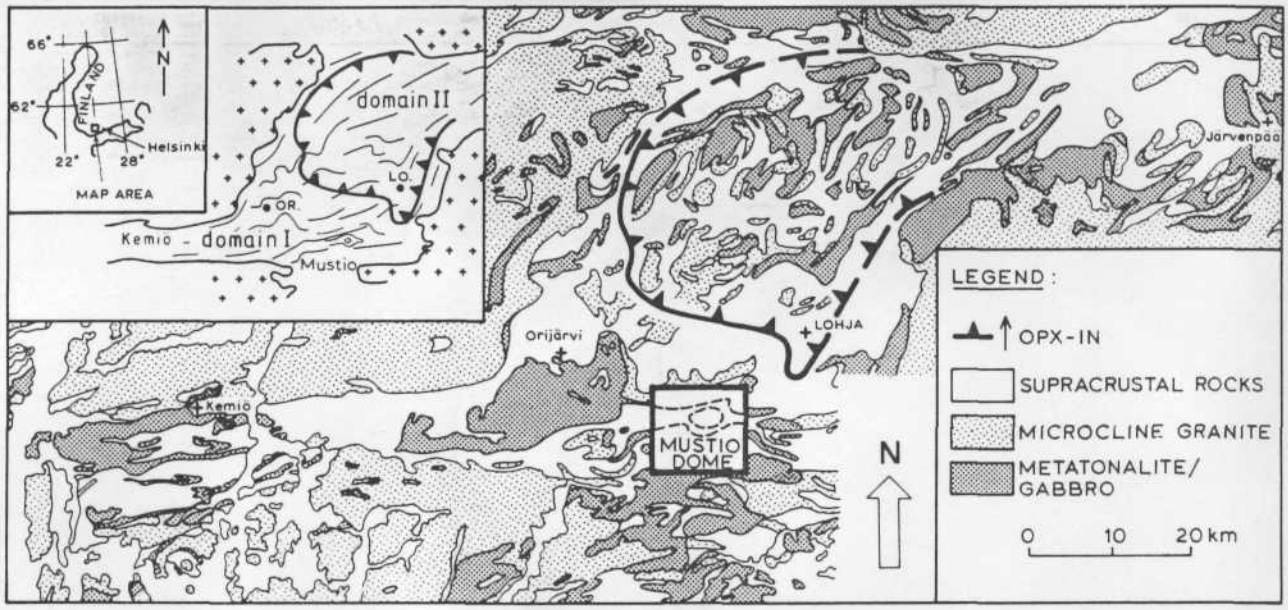

Fig. 3. Simplified geological map of the Kemiö–Orijärvi–Lohja–Järvenpää metamorphic belt of SW Finland. Note the position of the Mustio dome southwest of the town Lohja and outside the orthopyroxene-in isograd which limits the granulite facies area known as the West Uusimaa complex. Note the extensive microcline occurrence south of the Mustio dome. (After Bleeker and Westra, 1987).

(1987), the rocks of the Mustio area (Fig. 1) can be divided (from old to young) as follows:

- Quartzo-feldspathic schists and gneisses, consisting of fine to medium grained felsic rocks with low biotite content. They are interpreted as meta-arkoses. Intercalations occur of calc-silicate gneisses and marbles.
- Pre-kinematic tonalitic to granodioritic intrusives. They occur as conformable lenses of coarse grained biotite bearing orthogneisses.
- Mafic to intermediate metavolcanics. They are associated with the tonalites and comprise biotite-hornblende gneisses, layered amphibolites and massive amphibolites (which can reach ultramafic composition). They are interpreted as subaqueous volcanic sediments mixed with basaltic flows and associated pillow lavas.
- Metagreywackes, which consist of a quartz, plagioclase and biotite.
- Metapelites, consisting of quartz, plagioclase, biotite, K-feldspar and sillimanite. A gradually transition exists between the metagreywackes and pelites.

This entire sequence is intruded by microcline granites and pegmatites, both as sills and dikes. Microscopic relations between porphyroblasts and foliation development demonstrate that peak metamorphism and migmatisation occurred post-F_1 to early-F_2 (Bleeker and Westra, 1987; Bleeker, 1984).

Relations and pattern of structural elements

The investigation of the Mustio sink was focussed on the pattern of the following structural elements: bedding (S_0), main foliation (S_1) and F_1 fold axis or lineation ($L_{0\times1}$), F_2 axial plane or crenulation cleavage (S_2) and F_2 fold axis or lineation ($L_{1\times2}$), mineral lineation (L_{min}). The labelling S_1–$L_{1\times2}$ accounts for to the succession of structures established in each separate exposure and does not refer to regional events. The interpretation on the successive generation of structures on the scale of the entire area, will be discussed later.

Although altered by metamorphism, lithol-

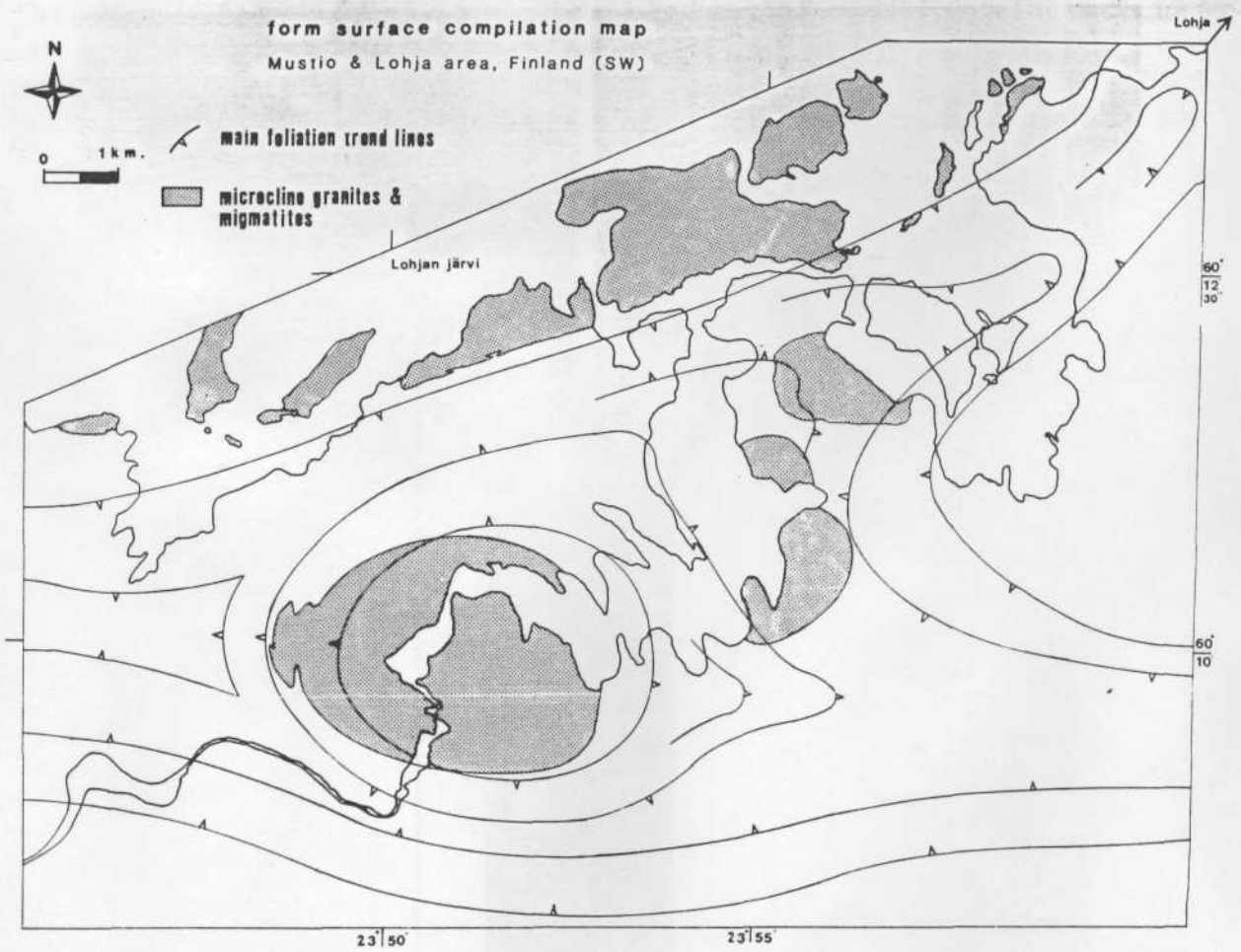

Fig. 4. Compilation from maps (of Bleeker and Westra, 1987 and Van den Kerkhof, 1980) of the Mustio and Lohja area. Indicated are the major outcrops of granites and migmatites. Below the southern edge of the map (not compiled), migmatitic and granitic bodies occur, striking E–W (see also Fig. 3). A complex cleavage-multiple-point occurs at the NE and E side of the Mustio dome. See text for further discussion.

ogical boundaries are still clearly visible in the pelitic and leptitic parts of the supracrustal series (Figs. 5A,B,D and E). Bedding is recognized by compositional variation on dm scale and sedimentary structures (e.g. convolute layering, Fig. 5A). The primary layering shows a distinct dome pattern (Fig. 1). The core of the dome consists of microcline granites and quartzofeldspathic schists and gneisses with marble intercalations. It is mantled by respectively an inner ring of mafic to intermediate meta-volcanics, a meta-pelitic ring, an outer volcanic ring and an outermost band of quartzofeldspathic rocks intercalated with marbles. The core of the gneiss dome shows anatectic structures (up to 30 percent melt products; Bleeker and Westra, 1987).

S_1 is defined by parallel alignment of biotite. It is parallel to the primary layering in intrafolial folds and sedimentary structures (Fig. 5A and B), as well as axial planar to regular, tight F_1 folds of S_0. Other F_1 fold types include:

– Open to tight, irregular parallel folds within metaclastic and pelitic rocks (Fig. 5E). These buckle folds developed without a cleavage. Hence, for reasons given at the beginning of this section, the folds are labeled F_1.

– Large open to tight, single, parallel folds of broken marble beds within pegmatitic sills (schematically drawn in Fig. 7B).


A

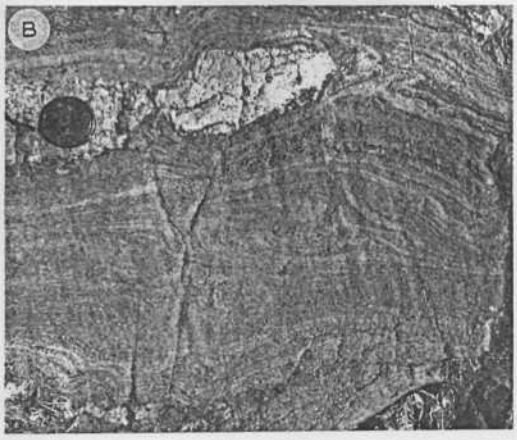
B

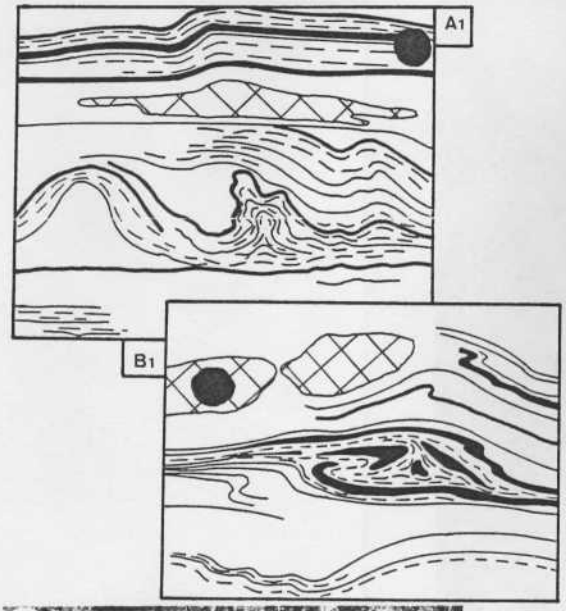
A1
B1


D


C

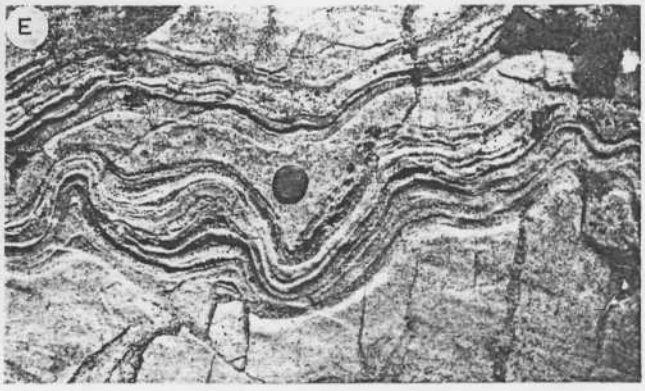
E

The pattern of the main foliation across the Mustio and Lohja area is shown in a compilation form surface map (Fig. 4, compiled from Bleeker and Westra, 1987; Van den Kerkhof, 1980). The pattern was studied in detail at the west side of the Mustio dome (Fig. 2). Figure 2 shows the west dipping flank of the dome while in the northwest the foliation dips southward to form a major synform with the north dipping limb in the southwest of the map. Hence the complete pattern is a triangular synform in which the foliation dips towards a central point, where the foliation is vertical. Such a structure is defined as a cleavage-triple-point (Brun et al., 1981).

$L_{0\times1}$ fold axes conform the trendlines of the limbs of the CTP and occur mostly on the flanks of the structure. The $L_{0\times1}$ on top of the dome is the fold axis of the broken-off marble bed mentioned above (Fig. 2, coordinates 491–6673), and its significance will be discussed later.

The orientation of S_2 has been interpreted as symmetry plane of regular F_2 folds. The angle between $L_{0\times1}$ and $L_{1\times2}$ can vary from 0° to >45° (Fig. 2, 487.1–6674.4). F_2 folding of S_1 occurs in:

– asymmetric folds to rootless isoclinal folds with transposed apices (Fig. 5B) in meta-arkosic beds. These folds are surrounded by unfolded stretched similar beds, and S_1 parallels both the folded and non-folded S_0 layering,

– tight is isoclinal similar folds of thin metapelitic layers within meta-arkosic layers (Fig. 5C). These intensively folded (S_0 and S_1) layers occur in stacks alternating with stacks in which the layers are non-folded (although in both stacks S_1 parallels S_0). The stacks are separated by granitic veins,

– open to tight, parallel, regular folds of 50 centimeter up to several meters, with crenulation cleavage (Fig. 5D).

When S_1 is folded, the F_2 axial plane is parallel or at a small angle with the general trend of S_1, on macroscopic scale. The pattern of the F_2 axial planes can be shown best by means of the $L_{1\times2}$ trend (Fig. 2). Following the outward dipping S_1 foliation of the dome, the plunge of $L_{1\times2}$ lies in a plane parallel to the enveloping surface of the dome, although the pitch of $L_{1\times2}$ varies in this plane. This variation, parallel to the strike of S_1, is seen in the opposite plunge at 489–6672.2 (less than 45° northward and more than 45° southward) and at 489.5–6671.9 (E and W plunge). The variation in plunge direction is horizontally expressed as rake angle with the S_1 foliation trend (60° at 489.5–6671.9). At the north and south flank of the CTP, $L_{1\times2}$ plunges both E and W, with small rake angles and amount of plunge varying from less than 45° to almost vertical (488.5–6671). In the center of the CTP, the rake between $L_{1\times2}$ and S_1 trend is almost 90°, thus plunging in the dip direction of S_1. The $L_{1\times2}$ shows undulation in a plane roughly coinciding with the shape of the dome and sink. Undulation of $L_{1\times2}$ implies a reorientation after development or non-cylindrical genesis. At 487–6671.5 the reorientation shows three $L_{1\times2}$ plunging WNW and ESE. These foldaxes share an S_2 plane with consistent NNE dip. In stereographic projection, these fold axes plot on a great-circle coinciding with the axial plane of F_2 folds. The folds are non-cylindrical cur-

Fig. 5. (A) Meta-volcanics with ball and pillow structures. (A_1) Detailed line drawing of (A) with S_0 (solid lines), S_1 (broken lines) and a granitic vein (hatched). Note the top and botom of the picture with a straight $S_1//S_0$ relationship, and the chaotic middle part in which S_1 parallels S_0 as well. No overprinting or axial cleavages occur. (B) Asymmetric isoclinal rootless fold of $S_1//S_0$ in meta-arkoses. (B_1) Detailed line drawing of (B) with line notation idem as A_1 (quartz boudins hatched). Note the foliation pattern in the folds and the different intensity of shearing of all the folds. (C) Isoclinal similar cascade folds of $S_1//S_0$, divided from a nonfolded strata (at the right side) by a granitic vein (hatched). (D) Isoclinal compressional F_2 folds of S_1 parallel to S_0 (which consists of quartzite layers with micaceous intercalations (dark band). Arrow indicates F_2 crenulated S_1 and S_0 (E) Buckle-folding of S_0 without cleavage development. Lens cap on each picture is 5 cm. wide. See text for discussion.

viplanar and, combined with the pattern of $L_{1\times2}$, they undulate along the flanks of the CTP with their S_2 axial plane conforming the CTP.

Mineral lineation is mainly defined by amphibole. At one location the long axes of amphiboles coincide with the X-axes of volcanic bombs, thus representing a stretching lineation. The general trend is a progressively steeper plunge towards the center of the CTP.

Interpretation

Foliation development and generation of fold structures

Figure 5A shows convolute layering in meta-volcanics. The bedding is inferred from compositional differences. A penetrative foliation is defined by alignment of metamorphic minerals, as can be seen best in the top of the picture. As mentioned earlier, this foliation parallels the primary layering in both the straight upper and bottom part, and in the chaotically folded central part. The intra-stratal character of the folds demonstrates that they either originated prior to solidification (e.g. synsedimentary) or under high-ductile, metamorphic conditions. The parallelism of S_1 both to folded and non-folded strata shows that S_1 developed along planes of preexisting, primary anisotropy (mimetic growth) and did not develop tectonically as axial plane cleavage in this exposure. We therefore interpret a synsedimentary origin of the convolution.

Figure 5B shows S_1 parallel to S_0 in the transposed apices of a shear fold and is not the axial-plane cleavage of the fold. This shows the absence of pervasive F_1 transposition affecting the entire bedding everywhere. More likely, flexural slip or differential flow causes locally both small and transposed dragfolds (Fig. 5B: transposition in the center versus small asymmetric folds in the surrounding layers), before or after S_1 was produced mimetically.

The pattern of $L_{1\times2}$ cannot be due to interference of successive folding phases. Refolding, either by active or passive folding, cannot explain the CTP itself, nor the undulation of $L_{1\times2}$ along the triangular CTP, if these elements are to be derived from pre-F_3, E–W striking, horizontal upright folds. Figure 6 shows the impossibility of forming a N–S plunging horizontal $L_{1\times2}$ by F_3 refolding, either through crossfolding (Fig. $6B_1$) or doming (Fig. $6B_2$). Non-cylindrical F_3 crossfolding will produce a dome structure flanked by an E and W plunging F_2 antiform with a straight E–W trend line of $L_{1\times2}$ across the midline of the dome. This is not shown by the actual pattern of $L_{1\times2}$ at the west side of the Mustio dome, east of the sink (Fig. 2, 489–6672, 73). F_3 doming will refold the $L_{1\times2}$ by passive rotation and can produce almost vertical N–S and E–W plunges of $L_{1\times2}$ if no circumferential stretching is allowed. If circumferential stretching occurred, the same pattern of $L_{1\times2}$ as in the case of crossfolding would arise (Dixon and Summers, 1983; Schwerdtner and

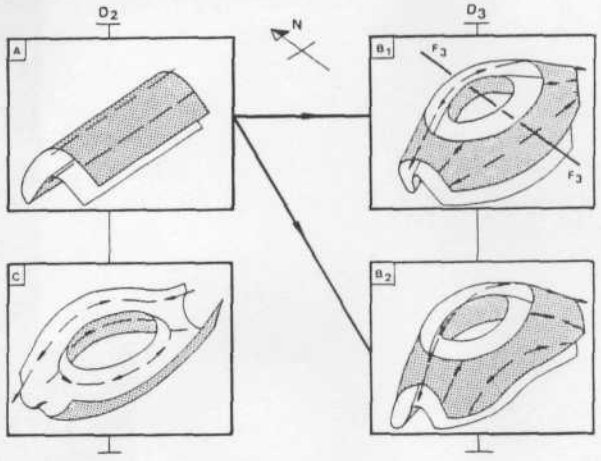

Fig. 6. Schematic pattern of the meta-volcanic band of Fig. 1 and the trajectories (foldaxes and lineations) of $L_{1\times2}$ are shown. Presumed F_3 refolding (B_1) or doming (B_2) from horizontal upright major F_2 folds (A) is set against single phase doming (C). Note the triangular map-pattern of the trajectories in the syn-F_2 sink. The axial symmetry of the S_0 implies F_3 refolding of an E–W striking F_2 antiform which consists of one major isoclinal recumbent E–W striking F_1 fold with the meta-pelites in its core (Bleeker and Westra, 1987). On the other hand, single phase doming implies a ring-syncline around the dome (Härme, 1953).

Troëng, 1978; Schwerdtner et al., 1978a, 1983). However, it will never rotate $L_{1\times2}$ towards N–S horizontal parallelism at the western edge of the dome, but will give a straight E–W trajectory across the midline. Therefore, no independent F_3 could have caused the pattern of $L_{1\times2}$; the origin of F_2 is interpreted to be syn-genetic with doming.

Model of the Mustio sink

In the Mustio area the three specific strain zones (Introduction and Fig. 8) of a CTP and dome structure are outlined by the distribution of the earlier described fold types and the foliation development.

Zone 1: At the top of the Mustio dome a horizontal flattening took place during the development of dome and sink. This produced penetrative tectonic S_1 development parallel S_0 with concurrent chocolate-bar boudinage in the foliation. The F_1 boudinaged and slumped structure of the marble of Figure 7B is situated on the crest of the Mustio dome. Although no folding should occur because of layer-parallel oblation, off-the-dome (spruce tree vergence) slumping of the marble bedding within a granitic sill can occur, due to loss of integrity of the marble within a low-viscosity medium (Talbot and Jackson, 1987).

Zone 2: At the flanks of the CTP, the strain field changes from horizontal to vertical oblation. As a result folding of the foliation fabric can develop in three ways:

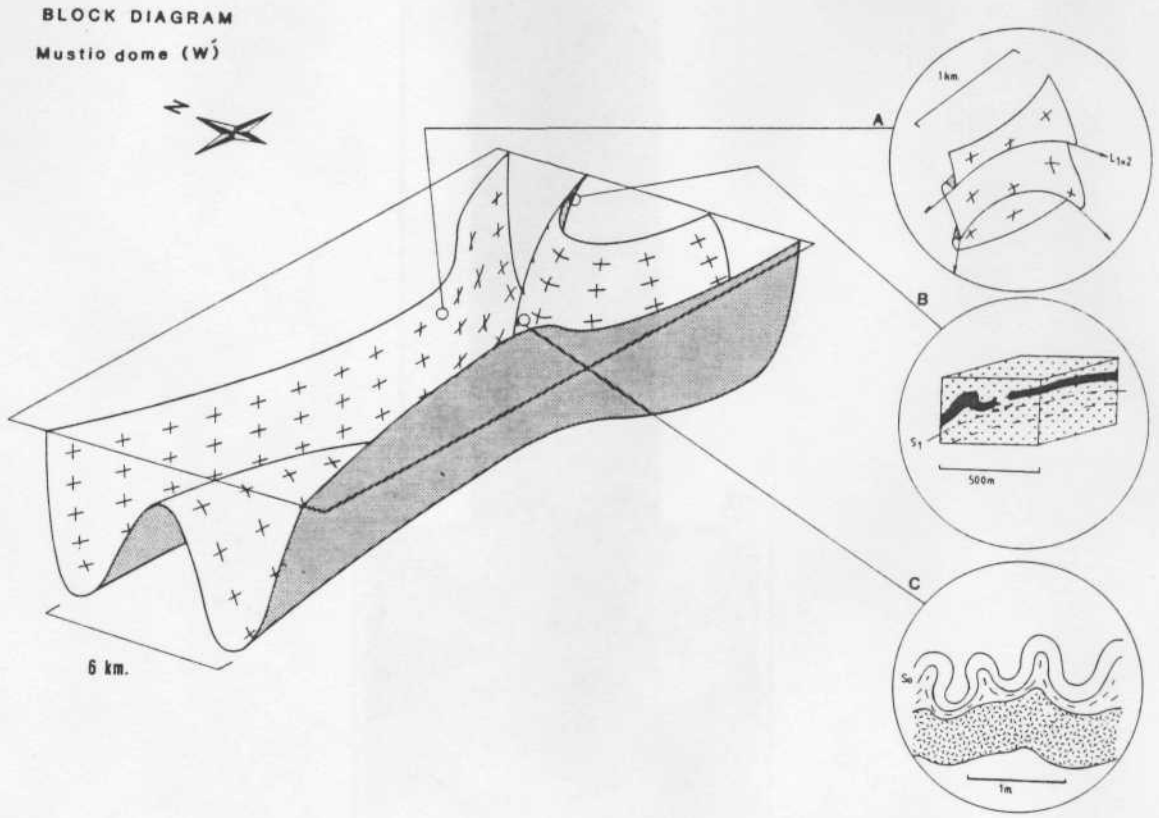

Fig. 7. Schematic block diagram of the Mustio dome and sink area. The drawn horizon represents the meta-volcanic band (see Fig. 1). As shown, single phase folding of the original layering can account for the outcrop pattern of the bedding at the Mustio dome. Inserts A–C schematically indicate the different F_1 and F_2 folding style and their location in the structure. Note that F_1 and F_2 factual relations in exposures. The anti- and synformal structure at the west side of the diagram (west of the Mustio sink) are an interpretation of the aeromagnetic-anomaly map, in accordance with Bleeker and Westra (1987). (Issued by the Geological Survey of Finland.)

– compressional folding (to-the-dome vergence) due to the transition of strain field, described above,
– cascade folds (off-the-dome vergence) due to decelerating flow downward (Dixon, 1975; Talbot and Jackson, 1987),
– shear folds (both vergences) due to differential subsidence (Dixon and Summers, 1983).

The tightness of the CTP defines the relative importance of the folding styles. However, all styles (Dixon and Summers, 1983) as well as both vergences of the folds can occur simultaneously. Within a migmatic pile of rocks the transition between a rising core and a subsiding cover will be diffuse. To-the-dome verging dragfolds (flexural slipfolds occur along thin bedding parallel neosomes, while off-the-dome (spruce tree) verging cascade and slump folds occur if a neosome reaches an extent that weakens or disconnects the layering (see also zone 1). The three folding styles can be recognized in the field. Figure 5B shows shear-folding at the south flank of the CTP. At 487-6674.4 (Fig. 2) an isoclinal fold (Fig 5D, with S_2 crenulation cleavage, is found. In the same exposure, cascade folds occur (Fig. 5C) which are separated from non-folded S_1 (parallel S_0) by a granitic vein, which acted as a decollement surface. Because migmatic veins may accomodate strain without recording it, they can form step-zones in intensity of folding.

All three fold types will develop with their fold axes initially circumferential parallel to the CTP flank, but as subsidence continuous, these axes rotate towards the dip direction of the flank to form sheath folds (Talbot and Jackson, 1987;). An undulating refolding is produced along the limbs of the CTP within one progressive deformation event. The curviplanar F_2 folds along the limbs of the Mustio sink can be explained in this way. The genera-

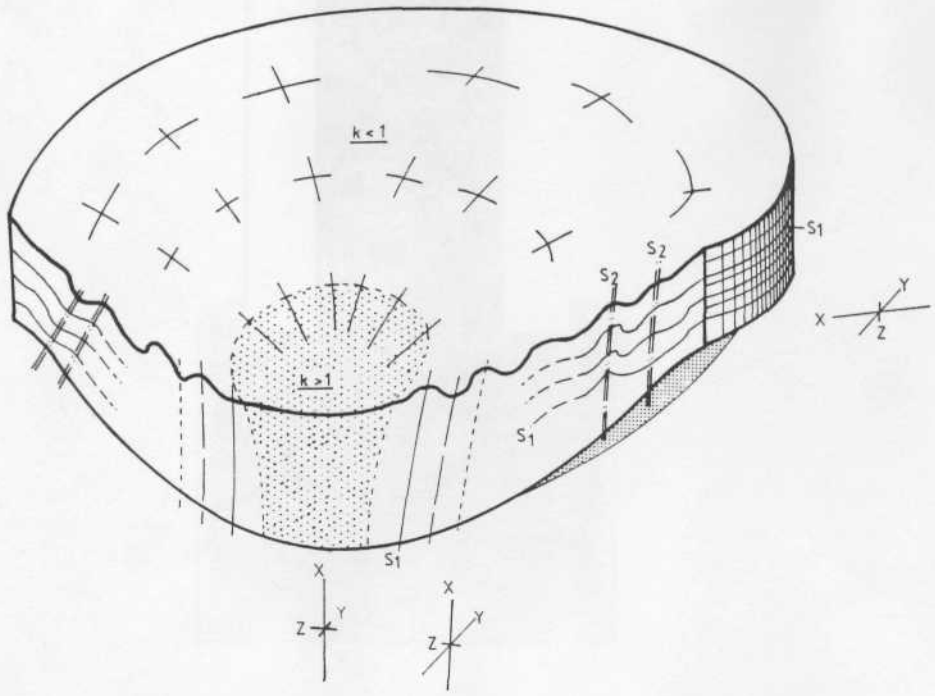

Fig. 8. Schematic model of a CTP structure and inter-domal sink surrounded by rising mobile bodies (not shown). Indicated are the strain zones and the orientation of the strain axes (from the rim to the center respectively: zones 1, 2 and 3). For further discussion see text.

tion of these three types of folds, as inferred from overprinting relationships in the field, can be complex due to the occurrence of S_1 in this zone as both mimetic and axial to folds). Figure 8 shows that only the distance between dome-centre and CTP controls overprinting relationships of the folds developed:
– near the dome, the cover is folded after a mimetic foliation developed due to a strong initial layer-parallel flattening strain in zone 1 (S_1 parallel to S_0 and F_2 axial plane);
– near the centre of the CTP, folding occurs without a previous strong layer-parallel flattening strain producing a layer parallel foliation (S_1 develops as axial plane to S_0).
Folding in the transition zone takes place due to the subsidence of the cover, but the fabrics which are folded may differ in age depending on where they originated, and not when.

Zone 3: In the center of the CTP initially the horizontally oblation was weakest or absent, being at the greatest distance from the granitic culminations. Almost at the beginning of the deformation history, horizontal bi-axial compression occurred, resulting into so-called curtainfolds (Talbot and Jackson, 1987) or vertical buckle folding without foliation development (Fig. 5E). Figure 7 shows a geometrical model of the Mustio sink and dome (in accordance with Härme, 1953), in which the sedimentary layering is schematically drawn together with the specific folding of the three zones described above.

Strain analysis

Both qualitatively and quantitatively, strain analysis has been carried out. The locations of strain analyses are indicated in Fig. 2; the results are shown in Fig. 9. We used four different methods of strain measurement: (1) the R_f/ϕ method (Ramsey and Huber, 1983) has been applied on primary volcanic bombs (analysis VII); (2) the center-to-center method (Hanna and Fry, 1979; Erslev, 1988) has been carried out on garnet porphyroblasts which grew pre-F_2 folding (Bleeker and Westra, 1987; analyses II, III, VIII); (3) the density distribution method (Fernandez, 1988) on planar and linear minerals (analysis V); and

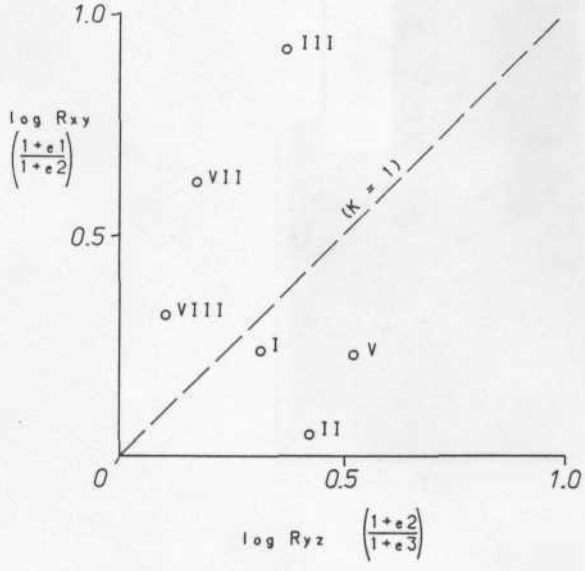

I : k = 0.75
X=256/44. XY-plane=340/84
II : k=0.06
X= 35/63. XY-plane= 8/66
III : k=5.38
X=298/27. XY-plane=341/36
IV : QUALITIVE ESTIMATE. Kf < 1
X=110/0. XY-plane=200/80
V : k=0.30
X= 40/24. XY-plane= 52/25
VI : QUALITIVE ESTIMATE. Kf < 1
X=355/85. XY-plane=355/85
VII : k=6.38
X=246/18. XY-plane=329/69
VIII: k=4.66
X=192/59. XY-plane=250/72

Fig. 9. Results of strain analyses I–VIII. A logarithmic scale is used on both X- and Y-axis. Orientation and *k*-value are shown in the table. For the locations see Fig. 2.

(4) the qualitative strain estimation of fabrics according to Schwerdtner et al. (1976) (analyses IV and VI). Except for method 1, all other methods have major restrictions on estimating the amount of strain (Veenhof, 19890. The methods have been used to indicate roughly the shape (i.e., constriction versus oblation) and orientation of the ellipsoid. When the CTP development is interpreted as one progressive deformation, the pattern (i.e., the shape and orientation) of the finite strain, throughout the deformation history, reflects the kinematic path of the sinking supracrustal rocks. Figure 8 shows the theoretical orientation and shape of the three principally different ellipsoids (Dixon and Summers, 1983). Except for analyses III and VII which point to circumferential stretching, all ellipsoids very well reflect the theoretical state of strain (Figs. 2, 8 and 9).

Discussion

Doming and associated deformational structures are still controversial (Coward, 1981; Van den Eeckhout et al., 1986; Talbot and Jackson, 1987; Paterson et al., 1989). In response to a rather general scenario of vertical tectonics (Eskola, 1949; Griffin, 1979) much attention has been paid to fold interference patterns for the origin of domes, in the Svecokarelides (Hopgood et al., 1976; Verhoef and Dietvorst, 1980; Van Staal and Williams, 1983; Park and Bowes, 1983; Ploegsma and Westra, 1989). Similarly Bleeker and Westra (1987) interpreted a successive folding history for the Mustio dome (Fig. 6*B*):

(1) a transposed bedding parallel S_1 and a large, recumbent, isoclinal, E–W striking fold (F_1) possibly related to an early phase of thrusting; (2) F_2 refolding of F_1 in a horizontal, upright, E–W striking fold; (3) refolding of F_2 along a N–S fold axis, to produce the domal structure (F_3). However, the pattern of mesoscopic fold axes described earlier, indicates that the Mustio dome is not an F_3 refolded major horizontal fold, but is formed (as dome) syngenetic with other major non-cylindrical folds, which strike E–W (Schreurs and Westra, 1986, who labeled these folds F_2) at the southern edge of the KOLJ belt (Figs. 3 and 4). This alternative interpretation of a single doming event solves the problem noted by Bleeker and Westra (1987) that any deformatial imprint of D_3 is lacking from the Mustio dome, because there is no other folding event except for doming itself.

The CTP model explains the highly variable fold styles, the ambivalent foliation development and the variable strain intensity. The model explains the (locally rootless0 refolding of the main foliation, developed parallel to S_0, without the necessity of invoking a long deformational period to transpose the S_0 parallel to S_1. These phenomena are controlled and limited by zones of progressively different heterogeneous strain of a CTP. Moreover, the model explains the non-coaxiality of $L_{0\times1}$ and $L_{1\times2}$, because the time and place of fold development is controlled by the differential subsidence (flow tectonics, Talbot and Jackson, 1987) and the geometry of the sink. A fold phase interference as outlined in Fig. 6B would result in a high degree of coaxiality between $L_{0\times1}$ and $L_{1\times2}$.

It is interesting to compare the present area with the Bergslagen region in central Sweden, which falls into the same tectonic provence. Oen (1987) and De Groot et al. (1988) interpreted several generations of anorogenic granitic plutons in an attenuated and rifted crust, causing gravity deformation of a soft volcanosedimentary cover. This eventually leads to folding in inter-diapir synclines. The Mustio area differs from Bergslagen in the amount of granite and the intensity of metamorphism, with both phenomena being higher. However, the granites in the Mustio area also lack any orogenic imprint because they triggered the deformation of the cover itself. Taking into account that most of the granite is migmatic, resemblance with the Bergslagen area is explained: a sedimentary cover softened by

migmatisation and granite injection will tectonically behave in a way comparable with soft sediment gravity deformation as postulated in Bergslagen.

Conclusions

From the presence of a cleavage-triple-point and the pattern of $L_{1\times2}$ it is concluded that the Mustio dome is not a result of successive interfering of independent fold phases. It developed simultaneously with regional large scale folds in a non-cylindrical folding mechanism.

The progressive and changing strain distribution inside a CTP is well expressed by the foliation and fold development of, and confirmed by strain analysis in the Mustio sink. It is therefore concluded that all deformation in the Mustio area is caused by a single-phase progressive event of an inter-domal synform. This doming and folding should therefore be labeled D_1 on a regional scale.

Acknowledgements

Dr. L. Westra and W. Bleeker are thanked for use of their geological field maps and figures which facilitated this investigation. Dr. C. Bierman, H. Helmers, Dr. A. van der Pluijm and one anonymous reviewer are thanked for reading the draft version of this paper and suggesting major improvements. We thank J.D. van Wees for helping us computing the Fernandez strain analysis.

References

Bateman, R., 1984. On the role of diapirism in the segregation, ascent and final emplacement of granitoid magmas. Tectonophysics, 110: 211–231.

Bateman, R., 1986. On the role of diapirism in the segregation, ascent and final emplacement of granitoid magmas – reply. Tectonophysics, 127: 167–169.

Bleeker, W., 1984. Fluid inclusions in two high grade quartz segregation from the Mustio area, Svecofennides SW Finland. Internal Rep. of the Free University, Amsterdam, unpublished.

Bleeker, W. and Westra, L., 1987. The evolution of the Mustio Gneiss Dome, Svecofennides of SW Finland. Precambrian Res., 36: 227–240.

Bowes, D.R., Halden, N.M., Koistinen, T.J. and Park, A.F., 1984. Structural features of basement and cover rocks in the eastern Svecokarelides, Finland. In: A. Kröner and R. Greiling (Editors), Precambrium Tectonics Illustrated. E. Schweizerbantsche Verlagsbuchhandlung, Stuttgart, 147–171.

Brun, J.P., Gapais, D. and Le Theoff, B., 1981. The mantled gneiss domes of Kuopio (Finland): Interfering diapirs. Tectonophysics, 74: 283–304.

Coward, M.P., 1981. Diapirism and gravity tectonics: Report of a Tectonic Studies Group Conf. held at Leeds University, 25–26 March 1980. J. Struct. Geol., 3(1): 89–95.

De Groot, P.A., Baker, J.H. and Oen, I.S., 1988. Evidence for gravity subsidence and granite diapirism in the 1.8–1.9 Ga Proterozoic succession of West Bergslagen, Sweden. Geol. Mijnbouw, 67(1): pp.

Dixon, J.M., 1975. Finite strain and progressive deformation in models of diapiric structures. Tectonophysics, 28: 89–124.

Dixon, J.M. and Summers, J.M., 1983. Patterns of total and incremental strain in subsiding troughs: experimental centrifuged models of interdiapir synclines. Can. J. Earth Sci., 20: 1843–1861.

Erslev, E.A., 1988. Normalized center-to-center strain analysis of packed aggregates. J. Struct. Geol., 10(2): 201–209.

Eskola, P., 1949., The problem of mantled gneiss domes. J. Geol. London, 104: 461–476.

Fernandez, A., 1988. Strain analysis from shape preferred orientation in magmatic rocks. Bull. Geol. Inst. Univ. Uppsala, N.S., 14, 806–807.

Gaal, G., 1982. Proterozoic evolution and late Svecokarelian plate deformation of the central Baltic shield. Geol. Rundschau, 71: 158–170.

Gaal, G. and Gorbatschev, R., 1987. An outline of the Precambrian evolution of the Baltic shield. Precambrian Res., 35: 15–52.

Gorman, B.E., Pearce, T.H. and Birkett, T.C., 1978. On the structure of Archaean Greenstone belts: Precambrian Res. 6: 23–41

Griffin, V.S., 1979. Diapirism, polydeformation and amoeboidal tectonic patterns in the Svecofennidic area of SW Finland. Tutkimusrapporti.

Hanna, S.S. and Fry, N., 1979. A comparison of methods of strain determination in rocks from SW Dyfed (Pembrokeshire) and adjacent areas, J. Struct. Geol., 1(2): 155.

Härme, M., 1953. Structure and stratigraphy of the Mustio area, southern Finland. Bull. Comm. Geol. Finland, 166: 29–48.

Hopgood, A.M., Bowes, D.R. and Addison, J., 1976. Structural development of migmatites near Skaldö, SW Finland. Bull. Geol. Soc. Finland, 48: 43–62.

Oen, I.S., 1987. Rift-related igneous activity and metallogenesis in SW Bergslagen, Sweden. Precambrian Res., 35: 367–382.

Park, A.F. and Bowes, D.R., 1983. Basement cover relationship during polyphase deformation in the Svecokarelides of the Kaavi district, E-Finland. Trans. R. Soc. Edinburgh Earth Sci., 74: 95–110.

Paterson, S.R., Vernon, R.H. and Tobisch, O.T., 1989. A review of criteria for the identification of magmatic and tectonic foliations in granitoids. J. Struct. Geol., 11: 349–363.

Ploegsma, M. and Westra, L., 1989. The early proterozoic Orijärvi triangle (SW Finland): a key area on the tectonic evolution of the Svecofennides. Precambrian Res., 47: 51–69.

Ramberg, H., 1981. Gravity, Deformation and the Earth's Crust: Theory, Experiments and Geological Application, 2nd ed., 425 Academic Press, London, pp.

Ramsay, J.G. and Huber, M.I., 1983. Techniques of Modern Structural Geology. 1. Strain Analysis. Academic Press, London.

Schreurs, J. and Westra, L., 1986. The thermotectonic evolution of a Proterozoic, low pressure, granulite, west Uusima, SW Finland. Contr. Min. Petrol., 93: 236–250.

Schwerdtner, W.M. and Troëng, B., 1978. Strain distribution within arcuate diapiric ridges of silicone putty. Tectonophysics, 50: 13–28.

Schwerdtner, W.M., Bennet, P.J. and Janes, T.W., 1976. Application of L–S fabric scheme to structural mapping and paleostrain analysis. Can. J. Earth Sci., 14: 1021–1032 (1977).

Schwerdtner, W.M., Suttcliff, R.H. and Troëng, B., 1978a. Patterns of total strain within the crestal region of immature diapirs: Can. J. Earth Sci., 15: 1437–1447.

Schwerdtner, W.M., Stott, G.M. and Suttcliffe, R.H., 1983. Strain patterns of crescentic granitoid plutons in the Archaean greenstone terrain of Ontario. J. Struct. Geol., 5(3/4): 419–430.

Simonen, A., 1980. The Precambrian in Finland. Geol Surv. Finland Bull., 304: 58 pp.

Talbot, C.J. and Jackson, M.P.A., 1987. Internal kinematics of Salt diapirs. Am. Ass. Petrol. Geol. Bull., 71(9): 185–202.

Van den Eeckhout, B., 1986. A case study of a mantled gneiss antiform, the Hospitalet Massif, Pyrenees (Andorra, France). PhD theses, Med. Inst. Aardw. State. State. Univ. Utrecht, 45.

Van den Eeckhout, B., Grocott, J. and Vissers, R., 1986. On the role of Diapirism in the segregation, ascent and final emplacement of granitoid magmas – discussion. Tectonophysics, 127, 161–166.

Van den Kerkhof, F., 1980. Geology of the Lohja area. Svecofennides of SW Finland. Internal Rep., Free University, Amsterdam, unpublished.

Van Staal, C.R. and Williams, P.F., 1983. Evolution of a Svecofennian mantled gneiss dome in SW Finland, with evidence for thrusting. Precambrian Res., 21: 101–128.

Veenhof, R.P., 1989. The Mustio sink (Svecofennides of SW Finland): a cleavage triple point and its mesoscopic structures. Internal Rep., Free University, Amsterdam, unpublished.

Verhoef, P.N.W. and Dietvorst, E.J.L., 1983. Structural analysis of differentiated schist and gneisses in the Taalintehdas area, Kemiö island, SW Finland. Bull.S Geol. Soc. Finland, 52: 147–164.